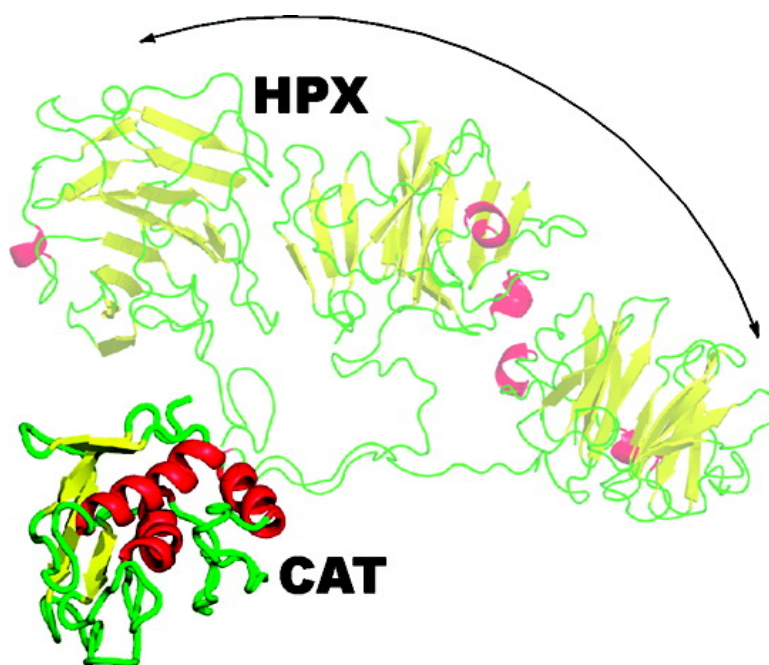Article

Evidence of Reciprocal Reorientation of the Catalytic and Hemopexin-Like Domains of Full-Length MMP-12

Ivano Bertini, Vito Calderone, Marco Fragai, Rahul Jaiswal, Claudio Luchinat, Maxime Melikian, Efstratios Mylonas, and Dmitri I. Svergun

More About This Article

Additional resources and features associated with this article are available within the HTML version:

- Supporting Information
- Links to the 1 articles that cite this article, as of the time of this article download
- Access to high resolution figures
- Links to articles and content related to this article
- Copyright permission to reproduce figures and/or text from this article

Evidence of Reciprocal Reorientation of the Catalytic and Hemopexin-Like Domains of Full-Length MMP-12

Ivano Bertini,*,[†,‡] Vito Calderone,[†] Marco Fragai,[†,§] Rahul Jaiswal,[†]
Claudio Luchinat,[†,§] Maxime Melikian,[†] Efstratios Mylonas,[‖] and Dmitri I. Svergun[‖,⊥]

*Magnetic Resonance Center (CERM), University of Florence, Via L. Sacconi 6, 50019 Sesto
Fiorentino, Italy, Department of Chemistry, University of Florence, Via della Lastruccia 3,
50019 Sesto Fiorentino, Italy, Department of Agricultural Biotechnology, University of Florence,
Via Maragliano, 75−77, 50144 Florence, Italy, European Molecular Biology Laboratory,
Hamburg Outstation, Notkestrasse 85, 22603 Hamburg, Germany, and Institute of
Crystallography, Russian Academy of Sciences, Leninsky pr. 59, 117333 Moscow, Russia*

Received November 20, 2007; E-mail: ivanobertini@cerm.unifi.it

Abstract: The proteolytic activity of matrix metalloproteinases toward extracellular matrix components (ECM), cytokines, chemokines, and membrane receptors is crucial for several homeostatic and pathological processes. Active MMPs are a family of single-chain enzymes (23 family members in the human genome), most of which constituted by a catalytic domain and by a hemopexin-like domain connected by a linker. The X-ray structures of MMP-1 and MMP-2 suggest a conserved and well-defined spatial relationship between the two domains. Here we present structural data for MMP-12, suitably stabilized against self-hydrolysis, both in solution (NMR and SAXS) and in the solid state (X-ray), showing that the hemopexin-like and the catalytic domains experience conformational freedom with respect to each other on a time scale shorter than 10^{-8} s. Hints on the probable conformations are also obtained. This experimental finding opens new perspectives for the often hypothesized active role of the hemopexin-like domain in the enzymatic activity of MMPs.

Introduction

Matrix metalloproteinases (MMP) are an important family of 23 proteins which are involved in a number of extracellular processes[1–3] including the degradation of the extracellular matrix.[4] The latter is constituted by structural proteins such as collagen and elastin, by proteoglycans, and by adhesive proteins such as fibronectin, laminin, and tenascin.[5] MMPs are single-chain enzymes secreted by cells as inactive proenzymes. The active form is liberated outside the cell by the cleavage of the prodomain by other proteases, including MMPs themselves,[6,7] thereby implying a complex regulation mechanism which also involves other proteins such as tissue inhibitors of MMPs (called TIMPs).[8,9]

All active MMPs but MMP-7 are constituted by two domains, a catalytic (CAT) and a hemopexin-like (HPX) domain. The CAT and HPX domains are connected by a linker whose length varies from 14 to 68 AA.[10,11] For many MMPs the linker is relatively short (14−23 AA) whereas for MMP-9 and MMP-15, at the other extreme, the intervening residues between the CAT and HPX domains (68 and 63 AA, respectively) constitute a further, highly glycosylated, domain termed OG domain.[12,13] The CAT domain alone bears full proteolytic activity toward a range of peptides and proteins.[14–17] However, efficient proteolysis of, for instance, triple helical collagen requires the full-

† CERM, University of Florence.
‡ Department of Chemistry, University of Florence.
§ Department of Agricultural Biotechnology, University of Florence.
‖ Hamburg Outstation.
⊥ Russian Academy of Sciences.

(1) Parks, W. C.; Wilson, C. L.; Lopez-Boado, Y. S. *Nat. Rev. Immunol.* **2004**, *4*, 617–629.
(2) D'Alessio, S.; Fibbi, G.; Cinelli, M.; Guiducci, S.; Del Rosso, A.; Margheri, F.; Serrati, S.; Pucci, M.; Kahaleh, B.; Fan, P. S.; Annunziato, F.; Cosmi, L.; Liotta, F.; Matucci-Cerinic, M.; Del Rosso, M. *Arthritis Rheum.* **2004**, *50*, 3275–3285.
(3) Boire, A.; Covic, L.; Agarwal, A.; Jacques, S.; Sherifl, S.; Kuliopulos, A. *Cell* **2005**, *120*, 303–313.
(4) Page-McCaw, A.; Ewald, A. J.; Werb, Z. *Nat. Rev. Mol. Cell Biol.* **2007**, *8*, 221–233.
(5) Aumailley, M.; Gayraud, B. *J. Mol. Med.* **1998**, *76*, 253–265.
(6) Knauper, V.; Will, H.; Lopez-Otin, C.; Smith, B.; Atkinson, S. J.; Stanton, H.; Hembry, R. M.; Murphy, G. *J. Biol. Chem.* **1996**, *271*, 17124–17131.
(7) Morrison, C. J.; Overall, C. M. *J. Biol. Chem.* **2006**, *281*, 26528–26539.

(8) Ra, H. J.; Parks, W. C. *Matrix Biol.* **2007**, *26*, 587–596.
(9) Overall, C. M.; Tam, E.; McQuibban, G. A.; Morrison, C.; Wallon, U. M.; Bigg, H. F.; King, A. E.; Roberts, C. R. *J. Biol. Chem.* **2000**, *275*, 39497–39506.
(10) Maskos, K.; Bode, W. *Mol. Biotechnol.* **2003**, *25*, 241–266.
(11) Andreini, C.; Banci, L.; Bertini, I.; Luchinat, C.; Rosato, A. *J. Proteome Res.* **2004**, *3*, 21–31.
(12) Van den Steen, P. E.; Grillet, B.; Opdenakker, G. *Glycobiol. Med.* **2005**, *564*, 45–55.
(13) Opdenakker, G.; Van den Steen, P. E.; Van Damme, J. *Trends Immunol.* **2001**, *22*, 571–579.
(14) Gronski, T. J.; Martin, R. L.; Kobayashi, D. K.; Walsh, B. C.; Holman, M. C.; Huber, M.; VanWart, H.; Shapiro, S. D. *J. Biol. Chem.* **1997**, *272*, 12189–12194.
(15) Mecham, R. P.; Broekelmann, T. J.; Fliszar, C. J.; Shapiro, S. D.; Welgus, H. G.; Senior, R. M. *J. Biol. Chem.* **1997**, *272*, 18071–18076.
(16) Murphy, G.; Allan, J. A.; Willenbrock, F.; Cockett, M. I.; O'Connell, J. P.; Docherty, A. J. *J. Biol. Chem.* **1992**, *267*, 9612–9618.

length active protein.[18,19] For this reason, it is often hypothesized that the HPX domain helps the local unwinding of the triple helix, in such a way that a single peptide strand can be accommodated in the active site of the CAT domain and cleaved.[20,21] It has been also hypothesized that a relative mobility of the HPX domain is necessary for this function.[22–25] This seems to be the case for MMP-9, for which small-angle X-ray scattering (SAXS) and atomic force microscopy (AFM) experiments indicate that the OG domain is able to lose its globular shape and transiently assume elongated structures, thereby allowing relative motion of the CAT and HPX domains.[26] On the other hand, X-ray structures of the full-length proenzyme forms of other MMPs lacking the OG domain display a well-defined structural relationship between the CAT and HPX domains, and this relationship is the same in the two different pro-MMPs studied (i.e., pro-MMP-1[25] (14 AA linker) and pro-MMP-2[27] (20 AA linker)).[25] The structures of active MMP-1,[28] and of its porcine ortholog,[29] are also compact and show a slightly different orientation of the HPX domain with respect to pro-MMP. This difference, although small, has been highlighted as evidence of the potential ability of the HPX domain to move with respect to the CAT domain.[25,28]

Here we have addressed the general problem of the relative conformational freedom of the two domains of MMPs in solution by NMR. NMR in solution is a powerful tool to investigate internal mobility of biomolecules[30–42] and can also provide precious information on interprotein and interdomain mobility.[43–49]

We selected MMP-12 (16 AA linker), for which an extended NMR assignment of the CAT domain is available, as well as high-resolution solid state and NMR structures. In this work, we have assigned the NMR signals of the HPX domain, solved its solution structure, and assigned the full-length protein. We have then obtained relaxation data (R_1, R_2, NOE) for the full-length protein and compared it with the same data for its isolated CAT and HPX domains. These data show that the two domains are not held rigidly to one another but must undergo independent motions. Residual dipolar couplings (RDC) on the full-length protein in the presence of an external orienting device were also obtained and found inconsistent with a rigid conformation of the protein.

Repeated attempts to crystallize full-length MMP-12 for X-ray diffraction finally yielded crystals of modest quality, which diffracted to 3 Å resolution. This low resolution was, however, largely sufficient to establish that the structure is less compact and the relative orientation of the two domains totally different, with respect to the four X-ray structures of MMP-1 and MMP-2 already described. Small-angle X-ray scattering (SAXS) data are consistent with the determined structure in the crystal representing the major conformation in solution but also point to a conformational mobility of the domains in MMP-12.[50]

Materials and Methods

Protein Expression. The cDNA encoding the G106-C470 sequence of full-length MMP-12 was generated by a polymerase chain reaction (PCR) from an IMAGE consortium clone using two synthetic oligonucleotides as primers. The cDNA obtained was cloned into the pET21a (Novagen) using the restriction enzymes *Nde I* and *Xho I* (New England BioLabs). One additional methionine at position 105 was present in the final expression product.

The expression vector encoding for the full-length protein (FL-MMP-12) was transformed into competent *Escherichia coli* BL21 (DE3) Codon Plus strain, and colonies were selected for Ampicillin and chloramphenicol resistance. Bacteria were grown in LB medium containing 34 μg/mL chloramphenicol and 50 μg/mL ampicillin in a shaker flask at 37 °C. Protein expression was induced with 0.5 mM IPTG at an $OD_{600} = 0.6$, and cell growth was continued for a further 5 h. For expression of ^{15}N and ^{13}C-enriched FL-MMP-12, the bacteria were grown in minimal medium containing ^{15}N enriched $(NH_4)_2SO_4$ and ^{13}C enriched glucose (Cambridge Isotope Laboratories). Cells were harvested by centrifugation and resuspended in a buffer containing 25% sucrose, 50 mM Tris-HCl (pH 8), 0.1 M NaCl, 0.2 M EDTA, 1 mM DTT. Five to ten milligrams of lysozyme were added to the resulting suspension and stirred for

(17) Overall, C. M.; McQuibban, G. A.; Clark-Lewis, I. *Biol. Chem.* **2002**, *383*, 1059–1066.

(18) Clark, I. E.; Cawston, T. E. *Biochem. J.* **1989**, *263*, 201–206.

(19) Ottl, J.; Gabriel, D.; Murphy, G.; Knauper, V.; Tominaga, Y.; Nagase, H.; Kroger, M.; Tschesche, H.; Bode, W.; Moroder, L. *Chem. Biol.* **2000**, *7*, 119–132.

(20) Chung, L. D.; Dinakarpandian, D.; Yoshida, N.; Lauer-Fields, J. L.; Fields, G. B.; Visse, R.; Nagase, H. *EMBO J.* **2004**, *23*, 3020–3030.

(21) Tam, E. M.; Moore, T. R.; Butler, G. S.; Overall, C. M. *J. Biol. Chem.* **2004**, *279*, 43336–43344.

(22) Gomis-Ruth, F. X.; Gohlke, U.; Betz, M.; Knauper, V.; Murphy, G.; Lopez-Otin, C.; Bode, W. *J. Mol. Biol.* **1996**, *264*, 556–566.

(23) de Souza, S. J.; Pereira, H. M.; Jacchieri, S.; Brentani, R. R. *FASEB J.* **1996**, *10*, 927–930.

(24) Overall, C. M. *Mol. Biotechnol.* **2002**, *22*, 51–86.

(25) Jozic, D.; Bourenkov, G.; Lim, N. H.; Visse, R.; Nagase, H.; Bode, W.; Maskos, K. *J. Biol. Chem.* **2005**, *280*, 9578–9585.

(26) Rosenblum, G.; Van den Steen, P. E.; Cohen, S. R.; Grossmann, J. G.; Frenkel, J.; Sertchook, R.; Slack, N.; Strange, R. W.; Opdenakker, G.; Sagi, I. *Structure* **2007**, *15*, 1227–1236.

(27) Morgunova, E.; Tuutila, A.; Bergmann, U.; Isupov, M.; Lindqvist, Y.; Schneider, G.; Tryggvason, K. *Science* **1999**, *284*, 1667–1670.

(28) Iyer, S.; Visse, R.; Nagase, H.; Acharya, K. R. *J. Mol. Biol.* **2006**, *362*, 78–88.

(29) Li, J.; Brick, P.; Ohare, M. C.; Skarzynski, T.; Lloyd, L. F.; Curry, V. A.; Clark, I. M.; Bigg, H. F.; Hazleman, B. L.; Cawston, T. E.; Blow, D. M. *Structure* **1995**, *3*, 541–549.

(30) Powers, R.; Clore, G. M.; Stahl, S. J.; Wingfield, P. T.; Gronenborn, A. M. *Biochemistry* **1992**, *31*, 9150–9157.

(31) Szyperski, T.; Luginbuhl, P.; Otting, G.; Güntert, P.; Wüthrich, K. *J. Biomol. NMR* **1993**, *3*, 151–164.

(32) Fischer, M. W. F.; Zeng, L.; Majumdar, A.; Zuiderweg, E. R. P. *Proc. Natl. Acad. Sci. U.S.A.* **1998**, *95*, 8016–8019.

(33) Ishima, R.; Torchia, D. A. *Nat. Struct. Biol.* **2000**, *7*, 740–743.

(34) Pfeiffer, S.; Fushman, D.; Cowburn, D. *J. Am. Chem. Soc.* **2001**, *123*, 3021–3026.

(35) Tolman, J. R.; Al-Hashimi, H. M.; Kay, L. E.; Prestegard, J. H. *J. Am. Chem. Soc.* **2001**, *123*, 1416–1424.

(36) Mulder, F. A. A.; Mittermaier, A.; Hon, B.; Dahlquist, F. W.; Kay, L. E. *Nat. Struct. Biol.* **2001**, *8*, 932–935.

(37) Eisenmesser, E. Z.; Bosco, D. A.; Akke, M.; Kern, D. *Science* **2002**, *295*, 1520–1523.

(38) Peti, W.; Meiler, J.; Brüschweiler, R.; Griesinger, C. *J. Am. Chem. Soc.* **2002**, *124*, 5822–5833.

(39) Bruschweiler, R. *Curr. Opin. Struct. Biol.* **2003**, *13*, 175–183.

(40) Lindorff-Larsen, K.; Best, R. B.; DePristo, M. A.; Dobson, C. M.; Vendruscolo, M. *Nature* **2005**, *433*, 128–132.

(41) Mittermaier, A.; Kay, L. E. *Science* **2006**, *312*, 224–228.

(42) Ferrage, F.; Pelupessy, P.; Cowburn, D.; Bodenhausen, G. *J. Am. Chem. Soc.* **2006**, *128*, 11072–11078.

(43) Barbato, G.; Ikura, M.; Kay, L. E.; Pastor, R. W.; Bax, A. *Biochemistry* **1992**, *31*, 5269–5278.

(44) Fischer, M. W.; Losonczi, J. A.; Weaver, J. L.; Prestegard, J. H. *Biochemistry* **1999**, *38*, 9013–9022.

(45) Baber, J. L.; Szabo, A.; Tjandra, N. *J. Am. Chem. Soc.* **2001**, *123*, 3953–3959.

(46) Jain, N. U.; Wyckoff, T. J. O.; Raetz, C. R. H.; Prestegard, J. H. *J. Mol. Biol.* **2004**, *343*, 1379–1389.

(47) Volkov, A. N.; Worrall, J. A. R.; Holtzmann, E.; Ubbink, M. *Proc. Natl. Acad. Sci. U.S.A.* **2006**, *103*, 18945–18950.

(48) Ryabov, Y. E.; Fushman, D. *Magn. Reson. Chem.* **2006**, *44*, S143–S151.

(49) Ryabov, Y. E.; Fushman, D. *J. Am. Chem. Soc.* **2007**, *129*, 3315–3327.

(50) Bertini, I.; Calderone, V.; Cosenza, M.; Fragai, M.; Lee, Y.-M.; Luchinat, C.; Mangani, S.; Terni, B.; Turano, P. *Proc. Natl. Acad. Sci. U.S.A.* **2005**, *102*, 5334–5339.

15−20 min at 4 °C. A buffer containing 2% Triton, 50 mM Tris-HCl (pH 8), 0.1 M NaCl, 0.2 M EDTA, and 1 mM DTT was added, and the suspension was sonicated (7−8 30 s cycles) and centrifuged at 40 000 rpm for 20 min at 4 °C. The pellets were resuspended in 6 M Urea, 20 mM Tris-HCl (pH 8) and centrifuged. The resulting inclusion bodies were solubilized in 6 M Gdn-HCl, 20 mM Tris-HCl (pH 8), 10 mM DTT, and 20 mM cystamine and stirred overnight at 4 °C. The insoluble material was removed by centrifuging at 9000 rpm for 10 min. Protein molecular weight and purity was checked on 15% gel by SDS-PAGE. The F171D, E219A mutant of FL-MMP-12 was produced using the quick-change site-directed mutagenesis kit (Qiagen), and the expression and purification of the protein and of its ^{15}N- and ^{13}C−^{15}N-enriched versions completed using the same procedure described above.

Refolding was carried out by a serial dilution method.[51] The protein was diluted to a final concentration of 0.13 mg/mL in 6 M Gdn-HCl, 20 mM Tris-HCl (pH 8), 1 mM DTT, and 0.05% Brij-35, stirred at 4 °C for 30−60 min, and dialyzed overnight against a buffer containing 20 mM Tris (pH 7.2), 10 mM CaCl$_2$, 0.1 mM ZnCl$_2$, 0.15 M NaCl, 5 mM β-mercaptoethanol, 1 mM 2-hydroxyethyl disulfide, and 0.05% Brij-35. The refolded protein was then purified using a Sepharose column (Amersham) with a buffer containing 20 mM Tris (pH 7.2), 10 mM CaCl$_2$, 0.3 M NaCl and 0.1 M acetohydroxamic acid (AHA). The protein solution was concentrated up to 5 mL and purified by size exclusion chromatography using a High Load 16/60 Superdex 75 (Amersham Biosciences) and eluted with 20 mM Tris pH 7.2, 10 mM CaCl$_2$, 0.3 M NaCl, and 0.2 M AHA. The eluted fractions were checked for purity on 15% gel by SDS-PAGE, and those containing the FL-MMP-12 protein were pooled and concentrated.

Samples of cadmium(II) substituted FL-MMP-12 protein were prepared by exhaustive dialysis against a buffer containing 20 mM Tris pH 7.2, 10 mM CaCl$_2$, 0.3 M NaCl, 0.2 M AHA, and 0.3 mM of CdCl$_2$.[52] Equimolar concentrations of *N*-isobutyl-*N*-[4methoxyphenylsulfonyl] glycyl hydroxamic acid (NNGH) were added to the samples to further increase the protein stability.

The cDNA encoding for the HPX domain (E278-C470) was generated by polymerase chain reaction and cloned into pET21a, using *Nde I* and *Xho I* as restriction enzymes. The expression vector was then transformed into competent *E. coli* BL21 (DE3) Gold strain, and the colonies were selected for Ampicillin resistance. Protein refolding for both nonlabeled and for ^{13}C and/or ^{15}N enriched samples was carried out by using the same protocols previously described for the preparation of FL-MMP-12 samples. Samples of the zinc(II) catalytic domain (F171D mutant) were prepared as previously described.[50]

NMR Measurements and Solution Structure Calculations. The experiments for the structure calculation and mobility measurements of the isolated HPX domain were performed on protein samples at concentrations ranging between 0.5 and 0.7 mM (pH 7.2). For FL-MMP-12, all NMR experiments were performed on samples at a concentration of 0.5 mM (pH 7.2).

All NMR experiments were performed at 298 K and acquired on Bruker AVANCE 900, AVANCE 800, AVANCE 700 and DRX 500 spectrometers. All instruments but one are equipped with triple resonance CRYO-probes. The 700 MHz spectrometer is equipped with a triple resonance (TXI) 5 mm probe with a *z*-axis pulse field gradient.

All spectra were processed with the Bruker TOPSPIN software packages and analyzed by the program CARA (Computer Aided Resonance Assignment, ETH Zürich).[53]

The backbone resonance assignment was obtained by the analysis of HNCA, HNCO, HN(CA)CO, HNCACB, and CBCA(CO)NH

spectra performed at 900 MHz. The assignment of the aliphatic side-chain resonances was performed through the analysis of 3D (H)CCH-TOCSY spectra at 500 MHz, together with 3D ^{15}N- and ^{13}C-NOESY-HSQC spectra at 900 MHz. The obtained assignments are reported in Tables S1 and S2 for the full length protein and tables S3 and S4 for the hemopexin domain. $^{3}J_{HNH\alpha}$ coupling constants were determined through the HNHA experiment at 500 MHz. Backbone dihedral φ angles were independently derived from $^{3}J_{HNH\alpha}$ coupling constants through the appropriate Karplus equation.[54] Backbone dihedral ψ angles for residue *i*-1 were also determined from the ratio of the intensities of the d$_{\alpha N}$(i-1,i) and d$_{N\alpha}$(i,i) NOEs present on the ^{15}N(*i*) plane of residue *i* obtained from the ^{15}N-edited NOESY-HSQC spectrum.

3D ^{15}N- and ^{13}C-enriched NOESY-HSQC cross peak intensities were integrated using the integration routine implemented in CARA and converted into interatomic upper distance limits by the program CALIBA.[55]

The protein assignment and the mobility measurements on FL-MMP-12 where performed on the NNGH-inhibited, cadmium(II)-substituted Phe171Asp/Glu219Ala mutant, due to its high stability to the self-hydrolysis. Mobility measurements on the catalytic domain where performed on the NNGH-inhibited, zinc(II) form of the Phe171Asp mutant.[50]

Residual dipolar couplings have been measured on FL-MMP-12 in the presence of an external orienting medium constituted by a binary mixture of C$_{12}$E$_5$ (penta-ethyleneglycol dodecyl ether, Fluka) and neat *n*-hexanol (Fluka), with a molar ratio C$_{12}$E$_5$/*n*-hexanol of 0.96 and with a C$_{12}$E$_5$/water ratio of 5 wt %.[56] One-bond ^{1}H−^{15}N coupling constants were measured at 298 K and 900 MHz by using the IPAP method.[57,58] Two-hundred fifty-nine rdc values could be measured that ranged from −46 to +25 Hz. Of them, only those rdc values corresponding to residues experiencing neither mobility nor large rmsd (140 residues, mostly in α or β secondary structures, see Table S5, Supporting Information) have been used for structure calculations and to investigate the reciprocal mobility of the two domains.

The program DYANA[59] was used to calculate a family of 1600 structures of the isolated HPX domain starting from randomly generated conformers in 20 000 annealing steps. The solution structure statistics are reported in Table S6 (Supporting Information). The family was energy-minimized by iterative cycles of DYANA with the program FANTAORIENT.[60] The quality of the structures calculated by DYANA can be assessed by a properly defined energy function (target function) proportional to the squared deviations of the calculated constraints from the experimental ones, plus the standard covalent and nonbonded energy terms. Structure calculation statistics and the structural quality were evaluated using the program PROCHECK_NMR.[61]

R$_1$, R$_2$, and NOE Measurements. The experiments for the determination of ^{15}N longitudinal and transverse relaxation rates and ^{1}H−^{15}N NOE were recorded at 298 K and 700 MHz on ^{15}N-enriched samples. The ^{15}N longitudinal relaxation rates (R_1) were measured using a sequence modified to remove cross correlation effects during the relaxation delay.[62] Inversion−recovery times

(54) Vuister, G. W.; Bax, A. *J. Am. Chem. Soc.* **1993**, *115*, 7772−7777.
(55) Guntert, P.; Braun, W.; Wüthrich, K. *J. Mol. Biol.* **1991**, *217*, 517−530.
(56) Rückert, M.; Otting, G. *J. Am. Chem. Soc.* **2000**, *122*, 7793−7797.
(57) Otting, G.; Ruckert, M.; Levitt, M. H.; Moshref, A. *J. Biomol. NMR* **2000**, *16*, 343−346.
(58) Ottiger, M.; Delaglio, F.; Bax, A. *J. Magn. Reson.* **1998**, *131*, 373−378.
(59) Guntert, P.; Mumenthaler, C.; Wüthrich, K. *J. Mol. Biol.* **1997**, *273*, 283−298.
(60) Bertini, I.; Luchinat, C.; Parigi, G. *Concepts Magn. Reson.* **2002**, *14*, 259−286.
(61) Laskowski, R. A.; Rullmann, J. A. C.; MacArthur, M. W.; Kaptein, R.; Thornton, J. M. *J. Biomol. NMR* **1996**, *8*, 477−486.
(62) Kay, L. E.; Nicholson, L. K.; Delaglio, F.; Bax, A.; Torchia, D. A. *J. Magn. Reson.* **1992**, *97*, 359−375.

(51) Bertini, I.; Calderone, V.; Fragai, M.; Luchinat, C.; Mangani, S.; Terni, B. *Angew. Chem. Int. Ed.* **2003**, *42*, 2673−2676.
(52) Bertini, I.; Fragai, M.; Lee, Y.-M.; Luchinat, C.; Terni, B. *Angew. Chem. Int. Ed.* **2004**, *43*, 2254−2256.
(53) Keller, R. L. J. The Computer Aided Resonance Assignment Tutorial, 1.3; Cantina: Verlag, 2004.

ranging between 2.5 and 3000 ms, with a recycle delay of 3.5 s, were used for the experiments. The ^{15}N transverse relaxation rates (R_2) were measured using a CPMG sequence[62,63] with delays ranging between 8.5 and 237.4 ms for the CAT domain, between 8.5 and 203.5 ms for the HPX domain, and finally between 8.5 and 135.7 ms for the FL-MMP-12 protein with a refocusing delay of 450 μs. The relaxation data are reported in Table S7 (Supporting Information). R_1 and R_2 data measured on the full length protein were found nosier and less uniform with respect to those of the single catalytic and hemopexin domains. This is related to the overlap of the signals in a so large protein and to the relative low solubility of the full length construct.

Crystallization, Data Collection, and X-ray Structure Determination. Crystals of the zinc(II) Phe171Asp/Glu219Ala FL-MMP-12 were obtained using the vapor diffusion technique at 20 °C from a solution containing 0.1 M Tris-HCl, 30% PEG-8000, 200 mM AHA, pH 8.0. The final protein concentration was 0.7 mM.

The data collection was carried out in-house, using a PX-Ultra copper sealed tube source (Oxford Diffraction) equipped with an Onyx CCD detector. The data set was collected at 100 K and the crystals used for data collection were cryo-cooled using a solution containing 10% ethylene glycol in the mother liquor.

The crystal diffracted to 3.0 Å resolution; it belongs to space-group C2 with one molecule in the asymmetric unit, a solvent content of about 50%, and a mosaicity of about 1.0°.

The data was processed using the program MOSFLM[64] and scaled using the program SCALA[65] with the TAILS and SEC-ONDARY corrections on (the latter restrained with a TIE SUR-FACE command) to achieve an empirical absorption correction. The structure was solved using the molecular replacement technique in two following steps; in the first step, the model used to find the correct orientation of the catalytic part of the structure was 1Y93 whereas the one used for the hemopexin domain was the same domain in proMMP-1 structure (1SU3). In both steps, inhibitors, water molecules, and ions were omitted from the models.

The correct orientation and translation of the molecules within the crystallographic unit cell was determined with standard Patterson search techniques[66,67] as implemented in the program MOLREP.[68,69] The isotropic refinement was carried out using REFMAC5[70] and default weights for the crystallographic term and the geometrical term were used.

In between the refinement cycles, the models were subjected to manual rebuilding by using XtalView.[71] The same program was used to model AHA molecule. Water molecules have been added by using the standard procedures within the ARP/WARP suite.[72] The stereochemical quality of the refined models was assessed using the program PROCHECK.[73] The Ramachandran plot is of average quality for such a resolution structure. Of the seven violations four (Asp303, Ser311, Lys315, and Asn363) are located in the hemopexin domain; it is interesting to compare these outliers to the equivalent residues in MMP-1 (1SU3) which has a higher resolution

(2.2 Å). Asp299 (corresponding to Asp303 in MMP-12) is an outlier as well, and in the place of Ser311 there is a proline residue (Pro307) which has of course a unique stereochemistry; furthermore in the place of Asn363 there is Gly359 in MMP-1, which again is unique from the stereochemical point of view. Therefore, three out of the four residues that are in disallowed regions in the HPX domain may actually assume peculiar positions in the 3-D structure. Table S8 (Supporting Information) reports the data collection and refinement statistics.

SAXS Experiments and Data Analysis. Synchrotron X-ray scattering data from solutions of the NNGH-inhibited, cadmium(II)-substituted Phe171Asp/Glu219Ala double mutant of FL-MMP-12 were collected on the X33 beamline of the EMBL (DESY, Hamburg),[74] using a MAR345 image plate detector. The scattering patterns were measured with a 2 min exposure time for several solute concentrations in the range from 0.8 to 8.3 mg/mL. To check for radiation damage, two 2 min exposures were compared, and no changes were detected. Using the sample−detector distance of 2.7 m, a range of momentum transfer of $0.01 < s < 0.5$ Å^{-1} was covered ($s = 4\pi \sin(\theta)/\lambda$, where 2θ is the scattering angle, and $\lambda = 1.5$ Å is the X-ray wavelength). The data were processed using standard procedures and extrapolated to infinite dilution using the program PRIMUS.[75] The forward scattering, $I(0)$, and the radius of gyration, R_g, were evaluated using the Guinier approximation,[76] assuming that at very small angles ($s < 1.3/R_g$) the intensity is represented as $I(s) = I(0) \exp(-(s^2 R_g^2)/3)$. The values of $I(0)$ and R_g, as well as the maximum dimension, D_{max}, and the interatomic distance distribution functions, $(p(r))$, were also computed using the program GNOM.[77] The molecular mass of FL-MMP-12 was evaluated by comparison of the forward scattering with that for a reference solution of bovine serum albumin (66 kDa).

The scattering from the high resolution models was computed using the program CRYSOL.[78] Given the atomic coordinates, the program either predicts the theoretical scattering pattern or fits the experimental intensity by adjusting the excluded volume of the particle and the contrast of the hydration layer to minimize the discrepancy

$$x^2 = \frac{1}{N-1} \sum_i \left[\frac{I_{exp}(S_j) - c I_{calc}(S_j)}{\sigma(S_j)} \right]^2 \qquad (1)$$

where N is the number of experimental points, c is a scaling factor, $I_{exp}(s_j)$ and $I_{calc}(s_j)$ are the experimental and calculated intensities, respectively, and $\sigma(s_j)$ is the experimental error at the momentum transfer s_j.

To assess the conformational variability of MMP-12, an ensemble optimization method (EOM) was used,[79] allowing for coexistence of multiple conformations in solution. About 5000 randomized models of MMP-12 differing by the conformation of the interdomain linker were generated using the program DYANA starting from randomly generated conformers of the full-length protein where only the dihedral angles of the linker region were left free to vary. These models formed a pool of possible structures, for which the scattering patterns were computed by CRYSOL. The EOM program employs a genetic algorithm to select from the pool a small number (usually about 20) of representative structures such that the average scattering from the selected ensemble fits the experimental data. Multiple runs of EOM were performed and the results were averaged to provide quantitative information about

(63) Peng, J. W.; Wagner, G. *Methods Enzymol.* **1994**, *239*, 563–596.
(64) Leslie, A. G. W. In *Molecular data processing*; Moras, D., Podjarny, A. D., Thierry, J.-C., Eds.; Oxford University Press: Oxford, 1991; pp 50−61.
(65) Evans, P. R. *Joint CCP4 and ESF-EACBM Newsletter* **1997**, *33*, 22–24.
(66) Rossmann, M. G.; Blow, D. M. *Acta Crystallogr.* **1962**, *15*, 24.
(67) Crowther, R. A. *The Molecular Replacement Method*; Rossmann, M. G., Ed.; Gordon & Breach: New York, 1972.
(68) Vagin, A.; Teplyakov, A. *J. Appl. Crystallogr.* **1997**, *30*, 1022–1025.
(69) Vagin, A.; Teplyakov, A. *Acta Crystallogr. D: Biol. Crystallogr.* **2000**, *56*, 1622–1624.
(70) Murshudov, G. N.; Vagin, A. A.; Dodson, E. J. *Acta Crystallogr.* **1997**, *D53*, 240–255.
(71) McRee, D. E. *J. Mol. Graphics* **1992**, *10*, 44–47.
(72) Lamzin, V. S. *Acta Crystallogr. D: Biol. Crystallogr.* **1993**, *49*, 129–147.
(73) Laskowski, R. A.; MacArthur, M. W.; Moss, D. S.; Thornton, J. M. *J. Appl. Crystallogr.* **1993**, *26*, 283–291.

(74) Roessle, M. W.; Klaering, R.; Ristau, U.; Robrahn, B.; Jahn, D.; Gehrmann, T.; Konarev, P. V.; Round, A.; Fiedler, S.; Hermes, S.; Svergun, D. I. *J. Appl. Crystallogr.* **2007**, *40*, s190–s194.
(75) Konarev, P. V.; Volkov, V. V.; Sokolova, A. V.; Koch, M. H. J.; Svergun, D. I. *J. Appl. Crystallogr.* **2003**, *36*, 1277–1282.
(76) Guinier, A. *Ann. Phys.* **1939**, *12*, 161–237.
(77) Svergun, D. I. *J. Appl. Crystallogr.* **1992**, *25*, 495–503.
(78) Svergun, D. I.; Barberato, C.; Koch, M. H. J. *J. Appl. Crystallogr.* **1995**, *28*, 768–773.
(79) Bernado, P.; Mylonas, E.; Petoukhov, M. V.; Blackledge, M.; Svergun, D. I. *J. Am. Chem. Soc.* **2007**, *129*, 5656–5664.

the flexibility of the protein in solution (in particular, about the R_g distribution in the selected ensembles).

Results and Discussion

Design and Production of a Stable Full-Length MMP-12. Several MMPs, both as isolated catalytic domains (CAT) or full-length (FL) proteins, are relatively unstable *in vitro* due to self-proteolysis (while the inactive isolated hemopexin domain (HPX) is stable). In the case of MMP-12, the CAT domain can be stabilized by a Phe171Asp mutation that prevents self-proteolysis and increases the solubility. This mutation is far both from the active site and from the CAT-HPX interface (see later) and does not perturb the catalytic activity of the enzyme. Therefore, a FL construct with the Phe171Asp mutation was initially produced. The resulting protein was well folded and fully active but still sensitive to the self-proteolysis at the linker region even in the presence of the inhibitor NNGH.

To increase the stability, the catalytically relevant Glu219 was mutated to an Ala. This mutation had been shown to decrease the catalytic activity of the isolated CAT domain of MMPs by two-3 orders of magnitude,[80] whereas the three-dimensional structure of the domain is fully retained.[81] The Phe171Asp/Glu219Ala double mutant of the FL protein was stable for several days.

Finally, we substituted the catalytic zinc(II) ion, responsible for the residual activity, with a cadmium(II) ion. The resulting derivative, complexed with NNGH, resulted stable to proteolysis, showing no trace of cleaved CAT and HPX domains in the gel after three weeks of NMR measurements. The analysis of the HSQC spectra revealed that no structural alteration were caused by the replacement of zinc(II) with the cadmium(II) ion.

The NNGH-inhibited, cadmium(II)-substituted Phe171Asp/ Glu219Ala double mutant of FL-MMP-12 was therefore used in all NMR experiments reported hereafter.

Low-Resolution X-Ray Structure of FL-MMP-12 and Comparison with Existing Structural Information on FL-MMP. Crystals diffracting at 3.0 Å were obtained for the AHA-inhibited, zinc(II) Phe171Asp/Glu219Ala double mutant of FL-MMP-12.

The X-ray structure of this construct was solved from diffraction data obtained in-house and deposited in PDB (PDB code: 3BA0). Despite the low resolution, the electron density was of generally good quality throughout the entire molecule, the only exception being residues 271−274 in the middle of the linker region (see below), which spans from Asp264 to Pro279. The overall structure of the CAT domain is very similar to the high resolution structure of the isolated CAT domain.[50] The mutations are both clearly visible; the active site contains both the native catalytic zinc ion and the structural zinc ion. Three calcium atoms are also present in the structure of the CAT domain. Finally, a AHA molecule bound to the zinc ion in the usual geometry[50] is present at the active site. The HPX domain has the expected four-blade propeller, hemopexin-like

fold previously observed in other HPX domains of MMPs.[22,25,27,29,82–85] The disulfide bridge between Cys282 and Cys470 is clearly present, and a calcium ion is bound in the central region of the domain.

The relative orientation of the two domains could be unambiguously determined from the 3 Å X-ray data (Figure 1A). The two domains are in contact through a relatively small surface (∼165 Å^2) which includes a possible salt bridge between His112 of CAT domain and the C-terminal of Cys470 in the HPX domain, and van der Waals interactions between residue 113 of CAT and residues 284 and 463 on the HPX side. The first part of the linker (residues 264, 265, 266, 270, 271, and 273) is in touch with the CAT domain (residues 112, 143, 144, 249, 259, and 263) through a surface of 902 Å^2 and the last part (residues 277 and 279) with the HPX domain (residues 280, 307, and 470) through a surface of 571 Å^2 (Figure 1A). Furthermore, the linker residue Lys266, besides being in contact with the CAT domain, forms a salt bridge with the C-terminal of HPX domain. The central part of the linker (residues 271−274) shows a rather poor electron density, but its structure can be reasonably modeled to match the arrangement of the initial and final linker residues. It is apparent that the whole molecule is held together mainly by interactions between each single domain and the linker rather than between the two domains. The presence of the intact linker was confirmed by a gel experiment on a protein solution obtained after redissolving crystals collected from the same wells of those used for X-ray.

Figure 1C shows a superposition of the X-ray structures of human proMMP-1 and proMMP-2, the only FL-proMMPs structures available to date, where the prodomain and the fibronectin domains (in case of MMP-2) have been omitted for clarity. The CAT-HPX interface is very similar in the two proteins and relatively extended (ca. 753 and 866 Å^2, respectively, as opposed to ca. 165 Å^2 in FL-MMP-12), suggestive of a stable domain-domain interaction. Figure 1D shows a superposition of the structures of active human FL-MMP-1[28] and of its porcine ortholog.[29] Again, the two structures are very similar, and the CAT-HPX interface is again extended (ca. 735 and 747 Å^2, respectively). The relative orientation of the HPX domain is slightly different in these active forms with respect to the pro-enzyme forms (cfr. Figure 1D and 1C, where the CAT domain has the same orientation), as previously noticed.[28]

Relative to the CAT domain, the HPX domain in FL-MMP-12 lies at about 120° with respect to its orientation in the structures of MMP-1 and MMP-2 (Figure 1E), and the two domains have a less compact arrangement (cfr. Figure 1A and 1B). The interface region is completely different, both viewed from the CAT and from the HPX domain, is sensibly smaller (ca. 165 vs 735−866 Å^2), and the complementarity between the surfaces of the two domains is poor with respect to that observed in the experimental structures of FL-MMP-1 and FL-MMP-2.

NMR Characterization of FL-MMP-12. The NNGH-inhibited, cadmium(II)-substituted Phe171Asp/Glu219Ala double mutant of FL-MMP-12 (FL-MMP-12 hereafter) yields $^{15}N-^1H$ HSQC spectra of surprisingly good quality for a protein of 42 000 Da (see Figure 2A) (spectra of this type were obtained on all constructs of FL-MMP-12 described before).

Figure 2B shows the $^{15}N-^1H$ HSQC spectrum of FL-MMP-12 (in black) superimposed to those of the isolated CAT domain (in green), prepared as previously reported, and of the isolated HPX domain (in red, see below). The similarity is striking: except for a number of peaks that are not present in either the

(80) Cha, J.; Auld, D. S. *Biochemistry* **1997**, *36*, 16019–16024.
(81) Bertini, I.; Calderone, V.; Fragai, M.; Luchinat, C.; Maletta, M.; Yeo, K. J. *Angew. Chem., Int. Ed.* **2006**, *45*, 7952–7955.
(82) Morgunova, E.; Tuuttila, A.; Bergmann, U.; Tryggvason, K. *Proc. Natl. Acad. Sci. U.S.A.* **2002**, *99*, 7414–7419.
(83) Libson, A. M.; Gittis, A. G.; Collier, I. E.; Marmer, B. L.; Goldberg, G. I.; Lattman, E. E. *Nat. Struct. Biol.* **1995**, *2*, 938–942.
(84) Gohlke, U.; Gomis-Ruth, F. X.; Crabbe, T.; Murphy, G.; Docherty, A. J.; Bode, W. *FEBS Lett.* **1996**, *378*, 126–130.
(85) Cha, H.; Kopetzki, E.; Huber, R.; Lanzendorfer, M.; Brandstetter, H. *J. Mol. Biol.* **2002**, *320*, 1065–1079.
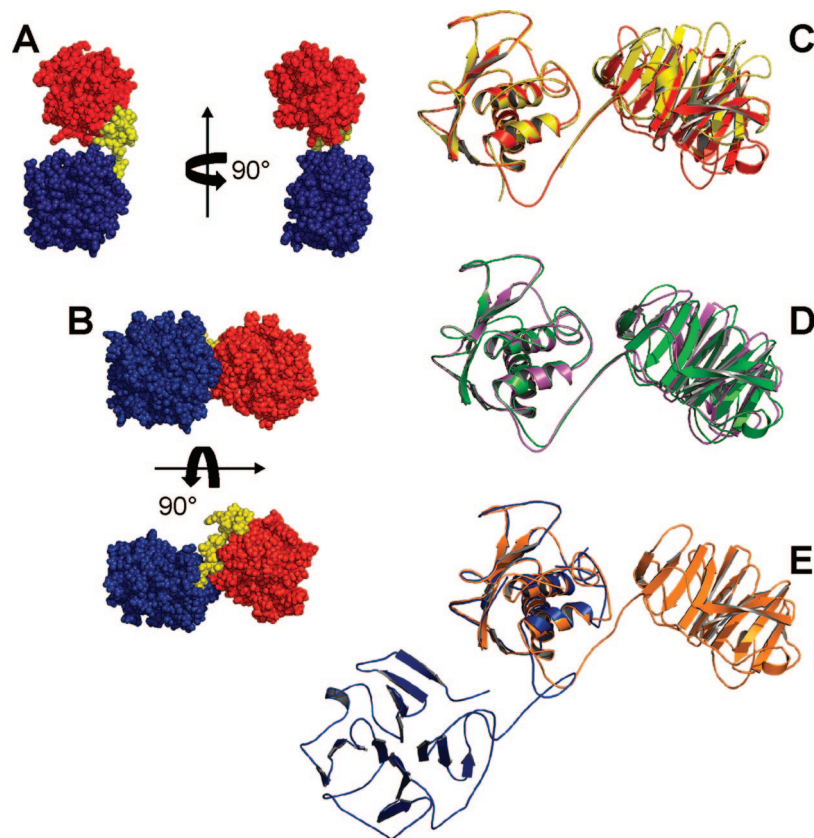
Figure 1. Space-filling representations of the X-ray structures of FL-MMP-12 (A, present work) and FL-MMP-1 (B).[28] Superimposition of the X-ray structures of (C) human pro-MMP-1[25] (red) and pro-MMP-2[27] (yellow) (where the prodomain of both and the fibronectin domains of MMP-2 have been omitted for clarity), (D) human[28] (violet) and porcine[29] (green) FL-MMP-1, and (E) human FL-MMP-1[28] (violet) with the present FL-MMP-12 (blue).

isolated CAT and HPX domains, which must therefore belong to the linker, all other FL-MMP-12 peaks are superimposable, or nearly superimposable, to a peak of either the isolated CAT or HPX domain. Furthermore, the peaks of FL-MMP-12 were only marginally broader that the corresponding peaks in the isolated domains.

The ^{13}C, ^{15}N, and ^{1}H spectral assignment of the CAT domain was available,[50] whereas that of the HPX domain was performed during this research. Also the solution structure of the HPX domain, up to now unavailable for MMP-12, was experimentally solved here (see Table S6 and Figure S1, Supporting Information) and deposited in PDB (PDB code: 2JXY). Ribbon representations of the solution and crystal structures are reported in Figure S1. The relatively high rmsd between the two structures (BB = 1.88 Å, secondary structure elements = 1.16 Å) is within the indetermination of both the X-ray (3.0 Å resolution) and NMR structures (BB rmsd = 1.38 Å, heavy atom rmsd = 2.13 Å).

The [15]N−^{1}H HSQC spectrum of FL-MMP-12 could be largely assigned by direct comparison with the isolated CAT and HPX spectra. Nevertheless, 97% of the nonlinker residues were reassigned by recording the same set of 3D spectra used for the structure of the isolated domains. Despite the crowding, the spectra were of good enough quality to assign most of the backbone atoms of the two domains as well as a large fraction of side-chain atoms (Table S1, Supporting Information). 3D NOESY spectra were also recorded. The NOESY patterns were largely the same as those observed in the isolated CAT and HPX domains, indicating that the domain structures are indeed unaltered in the FL protein, as it was already apparent from the comparison of the HSQC spectra. No interdomain NOEs could

be found. The largest difficulties in the assignment were encountered in the linker region. Although several of the linker [15]N−^{1}H HSQC peaks could be identified as the extra peaks present in the FL protein spectra and not corresponding to peaks of any of the two domains, several of the necessary sequential connectivities were missing in the 3D spectra. In addition, very few NOEs could be seen for these peaks. A protonless CON experiment[86] allowed us to identify two of the linker prolines. Ten linker peaks could be identified, and four of them sequence-specifically assigned (Table 1).

Relaxation Data. The 700 MHz R_1 and R_2 data for FL-MMP-12 as well as for the isolated CAT and HPX domains are shown in Figure 3A−D. R_1 and R_2 values can be accurately estimated from the atomic coordinates of a macromolecule of known structure assuming a rigid-body hydrodynamics by using computer programs like HYDRONMR.[87] In this study, the X-ray structure of the CAT domain (PDB code: 1Y93),[50] the present solution structure of the HPX domain, and the present X-ray structure of the full length protein (Figure 1E) were used as input files in HYDRONMR. As shown in Figure 3, while for the isolated domains the experimental data nicely match the calculated values, for FL-MMP-12 sizably faster longitudinal and sizably slower transverse relaxation rates with respect to the calculated values were measured. These differences are clearly statistically significant, despite the larger errors due to the signal overlap and lower signal-to-noise ratios in the spectra

(86) Bermel, W.; Bertini, I.; Duma, L.; Emsley, L.; Felli, I. C.; Pierattelli, R.; Vasos, P. R. *Angew. Chem., Int. Ed.* **2005**, *44*, 3089–3092.
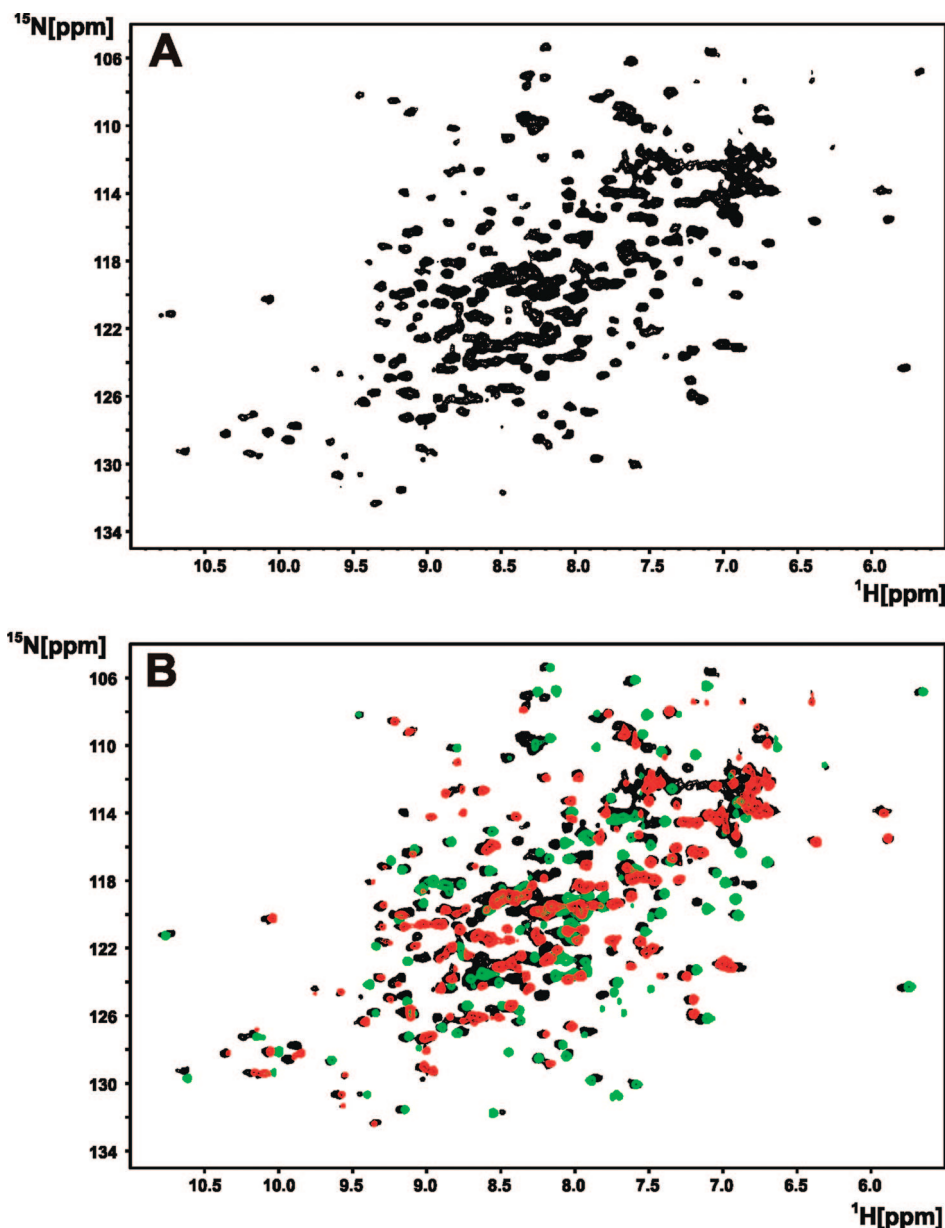(87) de la Torre, J. G.; Huertas, M. L.; Carrasco, B. *J. Magn. Reson.* **2000**, *147*, 138–146.

Figure 2. 900 MHz ^{15}N$-^1$H HSQC spectra of the uniformly ^{15}N-labelled NNGH-inhibited, cadmium(II)-substituted Phe171Asp/Glu219Ala double mutant of FL-MMP-12 (A), and superimposed spectra of FL-MMP-12 (black), CAT-MMP-12 (green), and HPX-MMP-12 (red) (B).

Table 1. ^{1}H, ^{15}N, and ^{13}C Chemical Shifts for the Identified Linker Residues of FL-MMP-12

		HN	N	CA	HA	CB	other	NOE
264	**D**	7.88	116.40	48.44	4.55	36.50	HB2 3.77, HB3 2.53	
272	**P**			60.17		29.20	CG 24.29, CD 46.96	
273	**N**	8.38	119.79	48.44	4.78	35.86	HB2 2.72, HB3 2.56	0.25
279	**P**			59.92	4.20	29.18	HB2 2.12, HB3 1.67, HG2 1.87, HG3 1.5, HD2 3.18, HD3 3.84	
L1		8.28	120.71	53.34	4.17	29.97	QB 1.78, CG 38.97, QG 2.87	
L2		8.17	109.42	57.03	4.83	39.62	HB2 3.05, HB3 2.60	
L3		7.89	122.58	49.62	4.18			
L4		8.16	121.91	53.24	4.19	30.91		0.28
L5		7.34	107.95	56.64				0.35
L6		8.37	123.69	51.65				

of FL-MMP-12. The R_1 and R_2 values measured on FL-MMP-12 are intermediate between the expectation from the isolated domains and a rigid full length structure. At the same time, the NOE values for FL-MMP-12 (Figure 3E) demonstrate that the single domains (catalytic and hemopexin) forming the full length protein behave as rigid bodies. Therefore, relaxation data can be collectively taken as evidence that the full length protein does not exhibit a rigid body hydrodynamics but experience flexibility. Such flexibility must depend on the presence of a flexible linker that permits sizable reciprocal mobility of the two domains on a time scale that is faster than the reorientation time of the whole molecule.
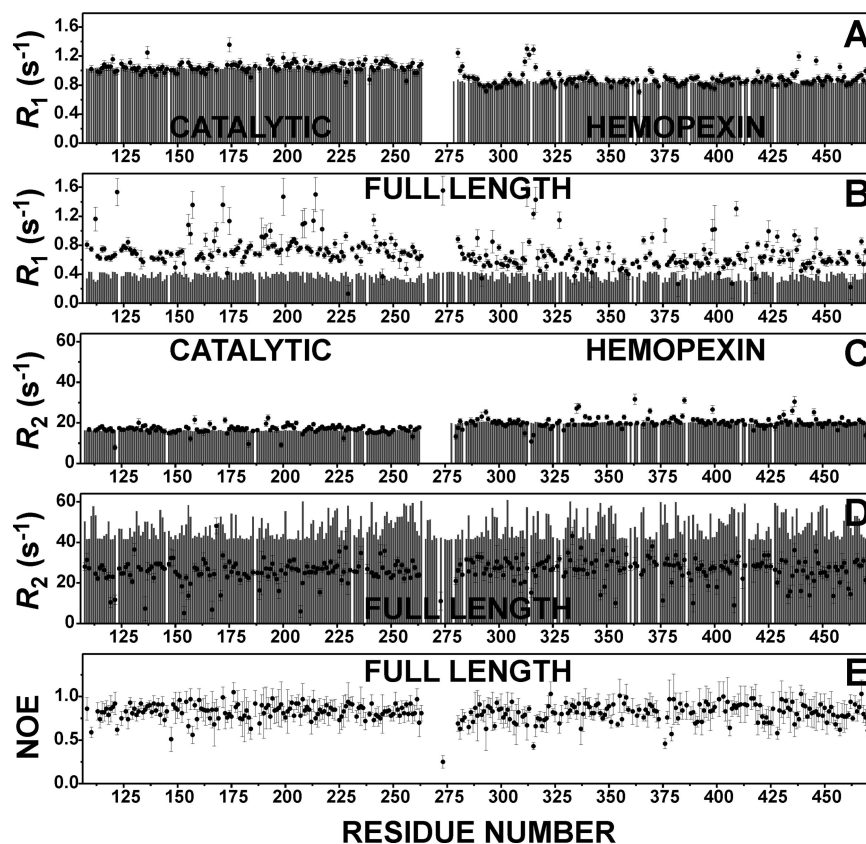
Figure 3. Calculated (grey bars) and experimental (filled circles) backbone ^{15}NH R_1 (A, B) and R_2 (C, D) values for the isolated CAT and HPX domains (A, C) and for the full-length protein (B, D). Although the agreement between experimental and calculated R_1 and R_2 values for the isolated domains is excellent, for the full-length protein the experimental R_1 values are sizably larger (B) and the R_2 values sizably smaller (D) than the ones calculated for the rigid X-ray structure. Experimental NOE values for the full-length protein (E).

Indeed, three linker peaks (N273, L4, L5) display grossly altered relaxation values, and particularly ^{15}N$-^1$H NOEs that are sizably smaller than expected (0.25, 0.28, and 0.35 respectively; Table 1). This is another indication that the linker is at least partially involved in some fast conformational rearrangement, consistent with a sizable degree of reciprocal mobility of the two domains. Incidentally, similar NOE values were observed in the linker region of calmodulin, a two-domain protein known to sample an extremely large conformational space,[43,45,50,88] and more recently in the two-domain xylanase Cex.[89] All R_1 and R_2 data on FL-MMP-12 and on its isolated CAT and HPX domains, together with NOE data, are reported in the Supporting Information (Table S7).

Residual Dipolar Couplings. Residual dipolar couplings (RDC) in the presence of the external orienting device C12E5/hexanol[56] have been measured. They can be fitted very well to the structures of the two isolated domains (Figure 4A,B) separately, but with sensibly different orientation tensor values. The data are, instead, in striking disagreement with the solid state X-ray structure (Figure 4C). Figure 4D shows that the agreement is modest also for any of the four rigid two-domain structures that can be obtained by fitting both domains to a single orientation tensor. None of these four structures bears a resemblance with the X-ray structure in terms of relative domain

orientation (Figure S2, Supporting Information). These structures are also different from any other X-ray structure of FL-MMPs. On this basis, and on the basis of the relaxation data, these solutions are discarded.

SAXS Experiments. The processed X-ray scattering pattern from FL-MMP-12 presented in Figure 5 yields a molar mass estimate of 40 ± 4 kDa, compatible with that calculated from the sequence (42.5 kDa), indicating that the protein is monomeric in solution. The experimental radius of gyration R_g and maximum size D_{max} are 31 ± 1 Å and 110 ± 10 Å, respectively. These values significantly exceed the parameters calculated from the X-ray structure of FL-MMP-1 ($R_g = 25$ Å, $D_{max} = 85$ Å), while they are in better agreement with those computed from the less compact X-ray structure of FL-MMP-12 determined in the present study ($R_g = 29$ Å, $D_{max} = 95$ Å). Moreover, the scattering pattern calculated from the FL-MMP-1 model using CRYSOL[78] fails to fit the experimental data (discrepancy $\chi = 5.8$, curve 2 in Figure 5).

The scattering curve computed from the present FL-MMP-12 structure displays a much better agreement to the experiment ($\chi = 2.5$, curve 3 in Figure 5), but still displays some systematic deviations. For flexible MMP-12, neither individual models, nor averaging over the random pool allowed one to fit the SAXS data. The representative ensembles selected to fit the data give information about the preferable conformations of the protein. Given the potential conformational flexibility of MMP-12 in solution suggested by the NMR data, an alternative analysis approach was applied, allowing for the coexistence of multiple protein configurations. A large number of models was generated

(88) Bertini, I.; Del Bianco, C.; Gelis, I.; Katsaros, N.; Luchinat, C.; Parigi, G.; Peana, M.; Provenzani, A.; Zoroddu, M. A. *Proc. Natl. Acad. Sci. U.S.A.* **2004**, *101*, 6841–6846.
(89) Poon, D. K. Y.; Withers, S. G.; McIntosh, L. P. *J. Biol. Chem.* **2007**, *282*, 2091–2100.
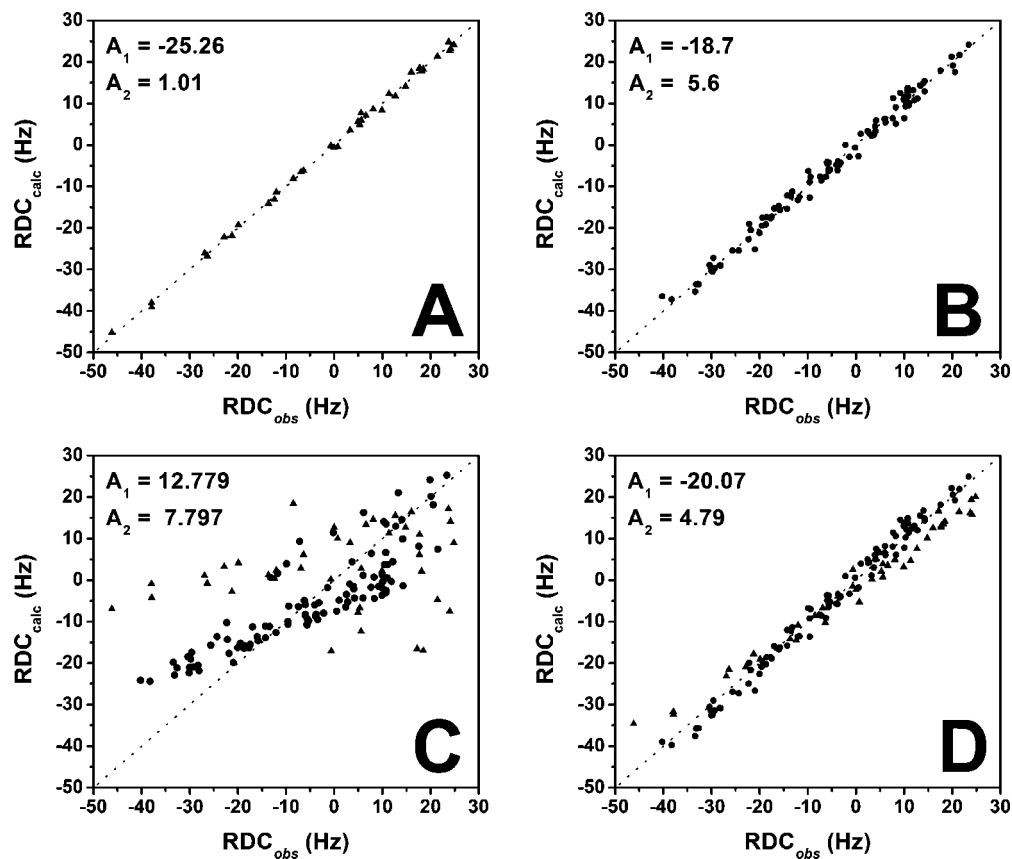
Figure 4. Best fit vs experimental 900 MHz RDC values for the NNGH-inhibited, cadmium(II)-substituted Phe171Asp/Glu219Ala double mutant of FL-MMP-12 in a binary mixture of $C_{12}E_5$ (penta-ethyleneglycol dodecyl ether) and neat n-hexanol. The separate fits for the CAT and the HPX domains and the best fit orientation tensor values are shown in A and B respectively. The poor global fit assuming the rigid X-ray structure is shown in C, and that obtained by best fitting the reciprocal orientation of the two domains to the RDC values is shown in D. In all panels, triangles refer to the CAT and filled circles refer to the HPX domain.

obtained by the linker randomizations representing possible conformations of MMP-12 in solution. None of these random models yielded a computed scattering in agreement with the experimental data. This was not unexpected, as SAXS "sees" the conformational and orientational average over the large (approx. 10^{16}) ensemble of protein molecules in the illuminated specimen volume. A simple average intensity of the generated pool also did not agree with the experiment, suggesting a nonrandom configuration of the linker in MMP-12. To assess the preferable conformations in solution, the EOM method[79] was used. Given a representative pool of (random) structures, the method employs a genetic algorithm to select the ensembles from this pool that best fit the experimental data, as explained in materials and methods. Several EOM runs yielded reproducible ensembles neatly fitting the experimental data with discrepancy χ in the range 1.1–1.3, and a typical fit provided by the ensemble selected by EOM is given in Figure 5, curve 4.

All the fits from different EOM runs are graphically indistinguishable from curve 4 in Figure 5.

The R_g distributions of the particles in the initial pool and in the selected ensembles are compared in the insert to Figure 5. The former distribution is rather broad, and covers the R_g range from about 23 to 50 Å, corresponding to extremely compact and completely extended domain configurations, respectively. In contrast, the R_g distribution of the selected ensembles displays a relatively sharp peak around $R_g = 28–29$ Å, including about 55% of the particles in the selected ensembles. Visual inspection of the models in the peak indicates,

not unexpectedly, that they have a shape similar to that of the MMP-12 structure in the crystal (although with varying interdomain orientations). In contrast, not a single structure with R_g < 27 Å was selected in multiple EOM reconstructions, indicating that models similar to the crystal structure of FL-MMP-1 were never present. These results indicate that the present crystal structure of FL-MMP-12 may be significantly present also in solution, but also that the protein experiences noticeable conformational flexibility, as revealed by the presence of a more or less uniform distribution of particles in the range between $R_g = 30$ and 50 Å and of a significant spike, which was always observed for the most extended particles (Figure 5, insert). We also tried to explore the possibility of a two-state exchange situation allowing for only two conformations in the mixture. The two-state fits were however always poorer than those from twenty-state EOM populations. In particular, by fixing the first state to be the crystal structure and allowing EOM to select the second state, discrepancies not better than 1.5–1.6 could be obtained. These results suggest that MMP12 adopts a manifold of conformations in solution, in full agreement with NMR observations.

Concluding Remarks and Biological Implications

The present data demonstrate that full-length MMP-12 shows relative mobility of its catalytic and hemopexin domains. The observation of R_1 and R_2 values intermediate between those of the isolated domains and those expected for any rigid structure of the full-length protein is particularly striking in this respect.
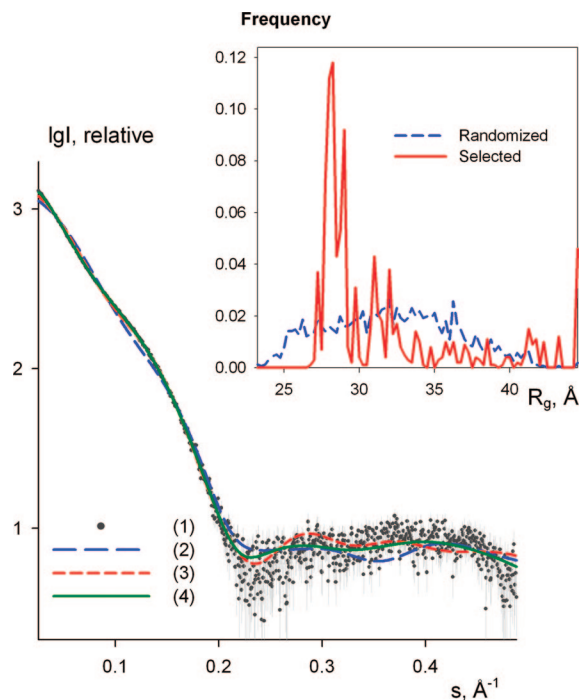
Figure 5. Experimental X-ray scattering from the NNGH-inhibited, cadmium(II)-substituted Phe171Asp/Glu219Ala double mutant of FL-MMP-12, and scattering from the models. (1) experimental data with error bars; (2−3) computed scattering from the crystallographic models of FL-MMP-1 and FL-MMP-12, respectively; (4) a typical fit by the selected ensemble of structures. The logarithm of the scattering intensity is plotted against the momentum transfer. Insert: the frequency of the models with the given R_g in the initial pool of structures with randomized interdomain linkers (blue broken line) and in the selected ensembles (red solid line); the latter distribution is obtained by the averaging of several EOM runs. Both R_g distributions are normalized to the integral value of unity.

Indeed, even in the case of calmodulin, the two-domain protein that constitutes a paradigmatic example of large interdomain mobility,[43,45,90,91] the R_1 and R_2 values are only modestly different from what expected for a rigid structure.[45,90] Apparently, in the case of FL-MMP-12 the reorientation of the backbone NH vectors with respect to the magnetic field occurs on a time scale that is faster than the rotational time of the whole molecule, whereas in calmodulin it is of the same order.[45,90] Conversely, the amplitude of the motion is probably lower for FL-MMP-12 than it is for calmodulin, as judged from the SAXS data that suggest that the molecules spend about half of the time in a conformation that is more or less as compact as the solid state structure. A similar behavior is probably experienced by the two-domain protein xylanase Cex, whose flexibility has been recently demonstrated.[89]

The present data are a significant example of the synergy between NMR and SAXS techniques.[92–96] NMR provides evidence of conformational freedom and of the time scale, whereas SAXS provides insight into the types and variety of the sampled conformations. About half of the conformations that are likely to be experienced by FL-MMP-12 in solution are as compact as the solid state structure but with different relative orientations of the two domains, while another half a re more extended, and some even highly extended. In this
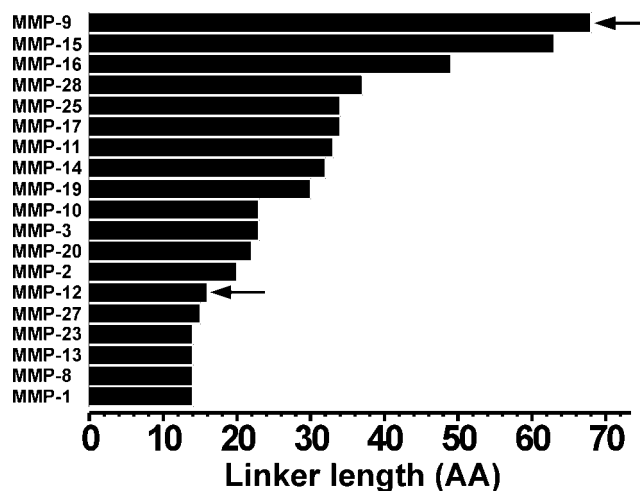

Figure 6. Linker lengths in matrix metalloproteinases. Arrows indicate MMPs for which interdomain mobility has been demonstrated (26 and present work).

respect the X-ray structure does not provide meaningful information on the conformation of the protein in solution.

Relative mobility of the CAT and HPX domains has been recently suggested for MMP-9, where the two domains are separated by the OG domain.[97] In the case of MMP-9 it has been argued[26] that the long and flexible OG domain may mediate protein−substrate interactions. Independent domain movements might even mediate enzyme translocation on a collagen fibril.[98,99] Another interesting possibility is that domain flexibility can mediate the activation of the enzyme and the cleavage of the pro-domain by promoting long-range conformational transitions induced by the binding of the activator proteins.[100] It is possible that MMP-12 can be representative of all other MMPs where the two domains are connected by a short linker rather than by a long one (Figure 6). However, this has to be demonstrated for those cases in which the contact area between the CAT and HPX domains is much larger than in the present case. Notably, the possibility of reorienting the hemopexin with respect to the catalytic domain during catalysis has been often invoked to rationalize the fact that, for collagenases (MMP-1, MMP8, and MMP-13), the catalytic domain alone is not able to attack collagen, whereas the full-length protein does.[18,19]

On the contrary, noncollagenase MMPs such as MMP-2 and MMP-12 do not degrade the native triple helix collagen. The

(90) Wang, T. Z.; Frederick, K. K.; Igumenova, T. I.; Wand, A. J.; Zuiderweg, E. R. P. *J. Am. Chem. Soc.* **2005**, *127*, 828–829.
(91) Bertini, I.; Gupta, Y. K.; Luchinat, C.; Parigi, G.; Peana, M.; Sgheri, L.; Yuan, J. *J. Am. Chem. Soc.* **2007**, *129*, 12786–12794.

(92) Mattinen, M. L.; Paakkonen, K.; Ikonen, T.; Craven, J.; Drakenberg, T.; Serimaa, R.; Waltho, J.; Annila, A. *Biophys. J.* **2002**, *83*, 1177–1183.
(93) Perry, A.; Tambyrajah, W.; Grossmann, J. G.; Lian, L. Y.; Scrutton, N. S. *Biochemistry* **2004**, *43*, 3167–3182.
(94) Grishaev, A.; Wu, J.; Trewhella, J.; Bax, A. *J. Am. Chem. Soc.* **2005**, *127*, 16621–16628.
(95) Marino, M.; Zou, P. J.; Svergun, D.; Garcia, P.; Edlich, C.; Simon, B.; Wilmanns, M.; Muhle-Gol, C.; Mayans, O. *Structure* **2006**, *14*, 1437–1447.
(96) Tsutakawa, S. E.; Hura, G. L.; Frankel, K. A.; Cooper, P. K.; Tainer, J. A. *J. Struct. Biol.* **2007**, *158*, 214–223.
(97) Van den Steen, P. E.; Van Aelst, I.; Hvidberg, V.; Piccard, H.; Fiten, P.; Jacobsen, C.; Moestrup, S. K.; Fry, S.; Royle, L.; Wormald, M. R.; Wallis, R.; Rudd, P. M.; Dwek, R. A.; Opdenakker, G. *J. Biol. Chem.* **2006**, *281*, 18626–18637.
(98) Overall, C. M.; Butler, G. S. *Structure* **2007**, *15*, 1159–1161.
(99) Saffarian, S.; Collier, I. E.; Marmer, B. L.; Elson, E. L.; Goldberg, G. *Science* **2004**, *306*, 108–111.
(100) Rosenblum, G.; Meroueh, S.; Toth, M.; Fisher, J. F.; Fridman, R.; Mobashery, S.; Sagi, I. *J. Am. Chem. Soc.* **2007**, *129*, 13566–13574.

real function of these noncollagenase proteins is still unknown. MMP-2 is able to degrade gelatin, a product of partial hydrolysis of collagen, and MMP-12 elastin, but we do not know if these are their real physiological roles. For MMP-12 it has been reported that the catalytic domain alone is able to degrade elastin even without the hemopexin domain. However, if during evolution the hemopexin domain has been maintained in spite of selective pressure, it is difficult to believe that it is useless. In this respect, the present discovery of relative mobility of the two domains in MMP-12 might be important for this still unknown function.

Supporting Information Available: NMR chemical shift values of FL-MMP-12 and of the hemopexin domain of MMP-12. The list of upper experimental constraints used for structure calculations. RDC values of FL-MMP-12. Statistical analysis of the NMR structures of the hemopexin domain of MMP-12. Relaxation data. Data collection, processing statistics, and refinement statistics for the crystallographic data set; Figure S1 and S2. This material is available free of charge via the Internet at http://pubs.acs.org.

JA710491Y